Radiology

ORIGINAL RESEARCH • CARDIAC IMAGING

# Comparison of Photon-counting Detector and Energy-integrating Detector CT for Visual Estimation of Coronary Percent Luminal Stenosis

*Cynthia H. McCollough, PhD • Prabhakar Rajiah, MD • John P. Bois, MD • Tim N. Winfree, MS • Rickey E. Carter, PhD • Kishore Rajendran, PhD • Eric E. Williamson, MD • Jamison E. Thorne, BS • Shuai Leng, PhD*

From the Department of Radiology, Mayo Clinic, 200 First St SW, Rochester, MN 55905 (C.H.M., P.R., J.P.B., T.N.W., K.R., E.E.W., J.E.T., S.L.); and Department of Health Science Research, Mayo Clinic, Jacksonville, Fla (R.E.C.). Received April 5, 2023; revision requested May 2; final revision received September 20; accepted October 20. **Address correspondence to** C.H.M. (email: *mccollough.cynthia@mayo.edu*).

Research reported in this article was supported by the National Institutes of Health under award number R01 EB028590. The content is solely the responsibility of the authors and does not necessarily represent the official views of the National Institutes of Health.

Conflicts of interest are listed at the end of this article.

See also the editorial by Murphy and Donnelly in this issue.

**Radiology 2023; 309(3):e230853 • https://doi.org/10.1148/radiol.230853 • Content codes: CA CT**

***Background:*** Compared with energy-integrating detector (EID) CT, the improved resolution of photon-counting detector (PCD) CT coupled with high-energy virtual monoenergetic images (VMIs) has been shown to decrease calcium blooming on images in phantoms and cadaveric specimens.

***Purpose:*** To determine the impact of dual-source PCD CT on visual and quantitative estimation of percent diameter luminal stenosis compared with dual-source EID CT in patients.

***Materials and Methods:*** This prospective study recruited consecutive adult patients from an outpatient facility between January and March 2022. Study participants underwent clinical dual-source EID coronary CT angiography followed by a research dual-source PCD CT examination. For PCD CT, multienergy data were used to create VMIs at 50 and 100 keV. Two readers independently reviewed EID CT images followed by PCD CT images after a washout period. Readers visually graded the most severe stenosis in terms of percent diameter luminal stenosis for the left main, left anterior descending, right, and circumflex coronary arteries, unblinded to scanner type. Quantitative measures of percent stenosis were made using commercial software. Visual and quantitative estimates of percent stenosis were compared between EID CT and PCD CT using the Wilcoxon signed-rank test.

***Results:*** A total of 25 participants (median age, 59 years [range, 18–78 years]; 16 male participants) were enrolled. On EID CT images, readers 1 and 2 identified 39 and 32 luminal stenoses, respectively, with a percent diameter luminal stenosis greater than 0%. Visual estimates of percent stenosis were lower on PCD CT images than EID CT images (reader 1: median 20.6% [IQR, 8.8%–61.2%] vs 31.8% [IQR, 12.9%–69.7%], $P < .001$; reader 2: 6.5% [IQR, 0.4%–54.1%] vs 22.9% [IQR, 1.8%–67.4%], $P = .002$). No difference was observed between EID CT and PCD CT for quantitative measures of percent stenosis (median difference, −1.5% [95% CI: −3.0%, 2.5%]; $P = .51$).

***Conclusion:*** Relative to using EID CT, using PCD CT led to decreases in visual estimates of percent stenosis.



After nearly a decade of preclinical work, energy-resolving photon-counting detector (PCD) CT became commercially available in 2021 (1,2). PCD CT has several benefits relative to energy-integrating detector (EID) CT (1,3–6). PCDs resolve the energy of detected photons and, with the use of a low energy threshold above the electronic noise level, are able to avoid the nonlinear increase in image noise at low detected dose levels. Further, PCD images exhibit increased bone and iodine enhancement relative to EID images, and PCDs can achieve spatial resolutions as good as 125 μm without the loss of geometric dose efficiency seen with EIDs (7–10). When PCDs are used in a dual-source geometry, the energy-resolved data allow cardiac multienergy imaging with a temporal resolution of 66 msec (2).

Coronary CT angiography provides minimally invasive imaging of coronary anatomy and is considered a first-line diagnostic tool in the setting of suspected coronary artery disease (11). Increased evidence of the value of coronary CT imaging from prospective multicenter trials has resulted in changes to clinical guidelines, most notably recommending its use during initial workup of cardiac symptoms, such as in patients presenting to the emergency department with chest pain (12). However, the presence of densely calcified plaque can severely limit the diagnostic value of the examination, with up to 11% of coronary CT angiograms rendered nondiagnostic (13,14).

Signal blooming is caused by insufficient spatial resolution in regions of high attenuation. Virtual monoenergetic images (VMIs) constructed using high photon energies (eg, 100 keV) demonstrate decreased calcium blooming because of the decreased attenuation of calcium at those energies. Hence, it is not surprising that the improved spatial resolution of PCD CT, coupled with the use of high-energy VMIs, has been shown in phantoms and cadaveric specimens to decrease blooming artifacts from calcified plaques compared with EID CT

### Abbreviations

CAD-RADS = Coronary Artery Disease Reporting and Data System, EID = energy-integrating detector, PCD = photon-counting detector, VMI = virtual monoenergetic image


### Summary

In patients clinically indicated for cardiac CT, photon-counting detector CT images demonstrated decreased calcium blooming compared with energy-integrating detector CT images, resulting in decreased visual estimates of percent diameter luminal stenosis.


### Key Results

- In 25 patients who underwent energy-integrating detector (EID) and photon-counting detector (PCD) CT, visual estimates of lumen stenosis were lower at PCD CT than EID CT (reader 1: median difference, −5.3%, $P < .001$; reader 2: median difference, −7.2%, $P = .002$).
- No difference was observed for quantitative estimates of lumen stenosis at PCD CT versus EID CT (median difference, −1.5%; $P = .51$).

(6,15–19). In these studies, PCD CT and high-energy VMIs have demonstrated more accurate quantification of calcified plaques relative to the reference standard. That is, the smaller percent diameter luminal stenosis values from PCD CT were always closer to the ground truth due to the reduction in calcium blooming. Initial experiences performing coronary CT angiography in patients using PCD CT have shown the promising potential of this novel technology (20–22). We hypothesize that, as in phantom studies, the percent diameter luminal stenosis at PCD CT will be lower than at EID CT. This prospective study aims to determine the impact of dual-source PCD CT on visual and quantitative estimations of percent diameter luminal stenosis compared with dual-source EID CT in patients clinically indicated for CT.

## Materials and Methods

### Participants

This prospective, institutional review board–approved, Health Insurance Portability and Accountability Act–compliant study recruited consecutive adult patients who underwent clinically indicated contrast-enhanced coronary CT angiography between January 2022 and March 2022. Participants were excluded if they were unable to provide informed consent, were pregnant, had an estimated glomerular filtration rate less than 60 mL/min/1.73 $m^2$, or had negative reactions to medications administered during the clinical EID CT examination (Fig 1). After written informed consent, a research PCD CT examination was performed on the same day.

### Imaging Procedures

EID CT scans were acquired using dual-source CT (SOMATOM Force; Siemens Healthineers) and our clinical protocol, which uses heart rate and indication to select the acquisition mode: adaptive prospectively triggered sequential mode with at least a 65%–75% acquisition window for patients with a heart rate less than 75 beats per minute and adaptive retrospectively gated spiral mode for patients with a heart rate of 75 beats per minute or greater or an unstable heart rate or when systolic imaging is indicated. Tube potential was automatically selected using CARE kV with the following settings: reference kilovoltage, 120; slider bar, 8; quality reference tube current–time product, 120 mA · sec; rotation time, 0.25 seconds; and collimation, 192 × 0.6 mm. Participants underwent PCD CT directly after EID CT.

PCD CT scans were acquired using a commercially available scanner (NAEOTOM Alpha, software version VA40; Siemens Healthineers) and an adaptive prospectively triggered sequential protocol with a 65%–75% acquisition window, 120 kV, CARE kV image quality level of 32, 0.25-second rotation time, and 144 × 0.4-mm collimation.

For both examinations, cardiac medications (5 mg of metoprolol [Lopressor; Hikma Pharmaceuticals] and 0.4 or 0.8 mg of nitroglycerin [Nitrostat; Pfizer] as a sublingual tablet) and contrast medium were administered per clinical routine. Iohexol at a concentration of 350 mg/mL (Omnipaque 350; GE HealthCare) was administered at an injection rate based on participant weight: less than 50 kg, 4 mL/sec; 50–100 kg, 5 mL/sec; and greater than 100 kg, 6 mL/sec. After the scan range was

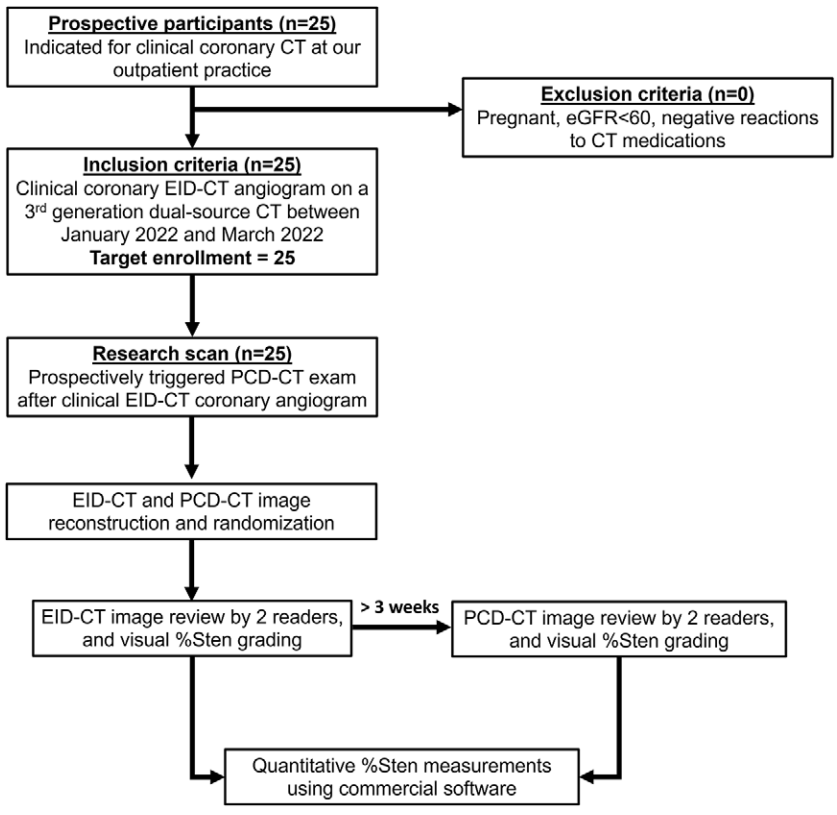


**Figure 1:** Study design flowchart. eGFR = estimated glomerular filtration rate, EID = energy-integrating detector, PCD = photon-counting detector, %Sten = percent diameter luminal stenosis.

prescribed, the scan time and postthreshold delay time (7 seconds) were summed to yield the injection time. Injection time was multiplied by the injection rate to determine the contrast medium volume for the first phase of the injection. The second phase consisted of a 40-mL mixture of 12 mL of contrast medium and 28 mL of 0.9% sodium chloride injected at the same rate, and the third phase of the injection consisted of 10 mL of 0.9% sodium chloride injected at the same rate. Bolus tracking was used to initiate the scan, with the monitoring region of interest placed over the ascending aorta and a trigger threshold of 150 HU at 120 kV.

### Image Reconstruction

Axial EID CT images were reconstructed using a medium-sharp vascular kernel (Bv40) and an iterative reconstruction strength level of 4 (Advanced Modeled Iterative Reconstruction; Siemens Healthineers), with a 0.6-mm section thickness and 0.3-mm increment. Axial PCD CT images were reconstructed using offline reconstruction software (ReconCT, version VA50; Siemens Healthineers) and a sharper vascular kernel (Bv48 for participants weighing >90 kg and Bv56 for participants weighing ≤90 kg), an iterative reconstruction strength level of 4 (Quantum Iterative Reconstruction; Siemens Healthineers), and a 0.4-mm section thickness and 0.2-mm increment. The modulation transfer function values at 2% for the Bv40 and Bv48 kernels were 8.02 and 9.36 line pairs per centimeter, respectively. Based on the literature and review of CT examinations not included in this study (23–25), VMIs were created at 50 keV and 100 keV; 50 keV was determined to provide substantial iodine enhancement without excessive noise amplification, and 100 keV was determined to provide a substantial decrease in calcium blooming without completely removing the iodine enhancement.

### Reader Estimation of Percent Diameter Luminal Stenosis

Two subspecialist cardiac imagers, a radiologist (P.R., with 13 years of experience) and a cardiologist (J.P.B., with 6 years of experience), independently read all studies in two sessions. The first session consisted of EID CT images, and the second session, which occurred a minimum of 3 weeks after the first session to mitigate observer memory bias, consisted of PCD CT images. Due to the obvious difference in spatial resolution and the presence of both 50- and 100-keV images from PCD CT, the readers were not blinded to scanner type. Readers were allowed to use the 50- and 100-keV images as they felt most appropriate to determine percent stenosis.

Percent stenosis was graded using a 17-cm visual analog scale anchored at 0% and 100%. No intermediate values were present on the scale. Readers drew a vertical line at the location most consistent with their perception of the stenosis. The markings were later measured with a ruler and were entered into the study database.

Grading was performed using our picture archiving and communication system (Visage 7; Visage Imaging), and readers were free to adjust display parameters and use multiplanar views. For the left main, right, left anterior descending, and circumflex coronary arteries, readers visually graded the most severe stenotic lesion in terms of percent stenosis without the use of digital calipers. Plaque attributes were not recorded, as this study focused on percent stenosis quantification. After grading stenosis severity for each artery, a single Coronary Artery Disease Reporting and Data System (CAD-RADS) score was assigned to the case using CAD-RADS version 1.0 (26). The EID CT–based score was subtracted from the PCD CT–based score such that negative values indicated a decrease in stenosis severity assessment with PCD CT.

### Quantitative Stenosis Measurement

Quantitative assessment of percent stenosis was performed by a CT technologist (with 8 years of experience) using commercial software (syngo.via, version VB70; Siemens Healthineers). For each participant, the most severe stenosis in each of the four main arteries was identified by visual inspection. The software segmented the coronary vessels, displayed them in curved multiplanar views, and automatically segmented the lumen along the coronary tree. The technologist placed a marker on the stenosis and at normal-appearing proximal and distal segments of the coronary artery, and the software calculated percent stenosis. Screenshots of the quantitative stenosis assessments were provided to the readers to indicate specific stenosis locations for their visual assessment. The averaged reader visual score was compared with the quantitative score for both EID and PCD CT images.

### Statistical Analysis

The analyses focused on estimating *(a)* the within-reader differences in percent stenosis ratings between EID CT and PCD CT images and *(b)* the interreader reliability separately for EID CT and PCD CT images. Continuous data are reported as means ± SDs or medians with IQRs. Categorical variables are reported as proportions with corresponding percentages. For within-reader between-modality comparisons, a minimum value of percent stenosis measured on EID CT images was implemented to exclude arteries without stenosis. In particular, the difference in percent stenosis at PCD CT versus EID CT for the lesions graded higher than 0% at EID CT was assessed using a Wilcoxon signed-rank test. This analysis accounted for the pairing between the EID CT and PCD CT images at the participant and artery level and was stratified by reader. If there were differences in the grading of lesions between readers, the paired set of arteries with lesions could vary between readers.

For the interreader reliability analysis, only arteries from participants in which at least one of the two readers graded the percent stenosis as 10% or higher on either the EID CT or PCD CT image were included. The 10% threshold was used to maximize the range of percent stenosis values included in the analysis while not artificially altering the agreement statistics by including a large number of arteries with no or minimal occlusions. Interreader reliability was estimated using the intraclass correlation coefficient under the assumption of a two-way random effect, and coefficients were interpreted according to previously published guidelines (27). Bland-Altman plots were also used to describe the agreement between the visual percent stenosis values. A Wilcoxon signed-rank test was used to test for differences in percent stenosis assessed quantitatively on EID CT versus PCD CT images.

In addition to the nonparametric test statistics, the Hodges-Lehmann estimator was used to estimate the median paired differences along with their 95% CIs. $P < 0.05$ was considered to indicate a statistically significant difference. Statistical analyses were performed by one author (R.E.C.) using R version 4.2.2 (R Foundation). For this pilot study, power calculations were not performed.

## Results

### Participant Characteristics

A total of 25 participants (median age, 59.5 years [IQR, 45.7–63.9 years]; 16 male participants, nine female participants) were enrolled, with no excluded participants (Fig 1, Table 1). For the EID CT scans, two of 25 (8%) participants were scanned in the dual-source adaptive prospectively triggered sequential scan mode, and 23 of 25 (92%) participants were scanned in the dual-source adaptive retrospectively gated scan mode. Due to the large number of EID CT examinations performed in the retrospectively gated scan mode for clinical indications (23 of 25 [92%] participants), the mean applied radiation dose (volume CT dose index) was 25.7 mGy ± 15.0 [SD]. Due to the use of the prospectively triggered scan mode at PCD CT, the mean volume CT dose index was lower, at 7.4 mGy ± 3.1.

**Table 1: Participant Characteristics**

| Variable | Value |
|---|---|
| Age (y) | |
| Median | 59.5 (45.7–63.9) |
| Range | 18–78 |
| Sex* | |
| M | 16 (64) |
| F | 9 (36) |
| Weight (kg) | |
| Median | 83.6 (72.3–94.9) |
| Range | 49.1–101 |

Note.—Except where indicated, data in parentheses are IQRs. Included participants ($n$ = 25) underwent energy-integrating detector CT and photon-counting detector CT.

* Data are numbers of participants, with percentages in parentheses.

### Reader Estimation of Percent Stenosis

On EID CT scans, reader 1 marked a total of 39 stenoses, with 20 of these having a visual percent stenosis of at least 30%. Reader 2 marked only 32 stenoses, of which only 14 had a percent stenosis of at least 30%.

Calcifications appeared smaller on 100-keV images from PCD CT due to improved spatial resolution and decreased calcium blooming. Figures 2 and 3 demonstrate the visual differences in stenotic lesions between EID CT and PCD CT images.

For both readers, median percent stenosis observed on PCD CT images was lower than that observed on EID CT images (reader 1: 20.6% [IQR, 8.8%–61.2%] vs 31.8% [IQR, 12.9%–69.7%], respectively, $P < .001$; reader 2: 6.5% [IQR, 0.4%–54.1%] vs 22.9% [IQR, 1.8%–67.4%], $P = .002$) (Table 2). The estimated median difference in percent stenosis between EID CT and PCD CT was −5.3% (95% CI: −7.6%, −3.5%) for reader 1 and −7.2% (95% CI: −11.5%, −2.2%) for reader 2. As shown in Figure 4, only a few lesions showed an increase in percent stenosis at PCD CT.

For reader 1, the CAD-RADS scores at PCD and EID CT did not differ for any of the 25 participants (zero of 25 [0%]). For reader 2, the CAD-RADS scores at PCD CT and EID CT did not differ for 18 of 25 (72%) participants and differed for seven of 25 (28%) participants. From EID CT to PCD CT, CAD-RADS scores decreased by one level in five of the 25 participants (20%), decreased by three levels in one participant (4%), and changed from a score of 1 to a score of N (nondiagnostic) in one participant (4%) due to a motion artifact.

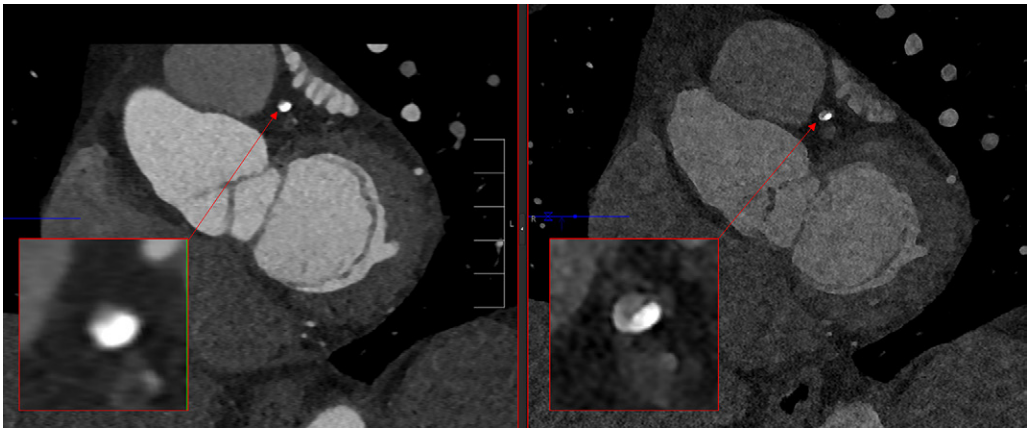

**Figure 2:** Axial images from an energy-integrating detector (EID) CT system (left) and a photon-counting detector (PCD) CT system at 100 keV (right) in a 63-year-old male participant referred for clinical coronary CT angiography. In the left main artery (inset enlarged images), the calcium is less bright and the lumen appears larger on the 100-keV PCD CT image, whereas the visible lumen on the EID CT image is relatively small due to calcium blooming (inset images). The visual percent diameter luminal stenosis estimate was 95% based on the EID CT image and 60% based on the PCD CT image. Window width was 500 HU and window level was 1500 HU for EID and PCD CT.

### Interreader Reliability

The intraclass correlation for the readers' estimation of percent stenosis was moderate, with coefficients of 0.64 (95% CI: 0.40, 0.80) at EID CT and 0.69 (95% CI: 0.45, 0.84) at PCD CT. Bland-Altman analyses (Fig 5) showed some systematic differences between the readers. The mean difference between readers was −6.8% (95% limits of agreement: −60.3% to 46.7%) for EID CT and −10.3% (95% limits of agreement: −55.6% to

35.0%) for PCD CT. The percent stenosis ratings by reader 2 were lower than those of reader 1 at PCD CT ($P$ = .01), but no difference was observed at EID CT ($P$ = .06).

### Quantitative Stenosis Measurement

A total of 18 stenoses were identified where the location of the stenosis had a clear match between the EID CT image and the 100-keV image from PCD CT. The percent stenosis values were lower at PCD CT than at EID CT for 12 of these 18 stenoses (66%), were equivalent for both techniques for one stenosis (5%), and were greater at PCD CT than at EID CT for five stenoses (28%) (Fig 6). No difference in mean and median percent stenosis was observed between EID CT (mean, 23.8% ± 10.1; median, 21.0% [IQR, 18.2%–28.0%]) and PCD CT (mean, 23.4% ± 11.9; median, 20.5% [IQR, 14.5%–29.7%]). The Hodges-Lehmann estimate of the difference in medians was −1.5% (95% CI: −3.0%, 2.5%; $P$ = .51). Visual estimation of percent stenosis severity in these same 18 stenoses, averaged across readers, showed that visual ratings based on EID CT images overestimated percent stenosis (mean, 35.4% ± 20.2; median, 35.0% [IQR, 23.1%–44.4%]; $P$ = .001) relative to the quantitative values, but no difference was found between the quantitative

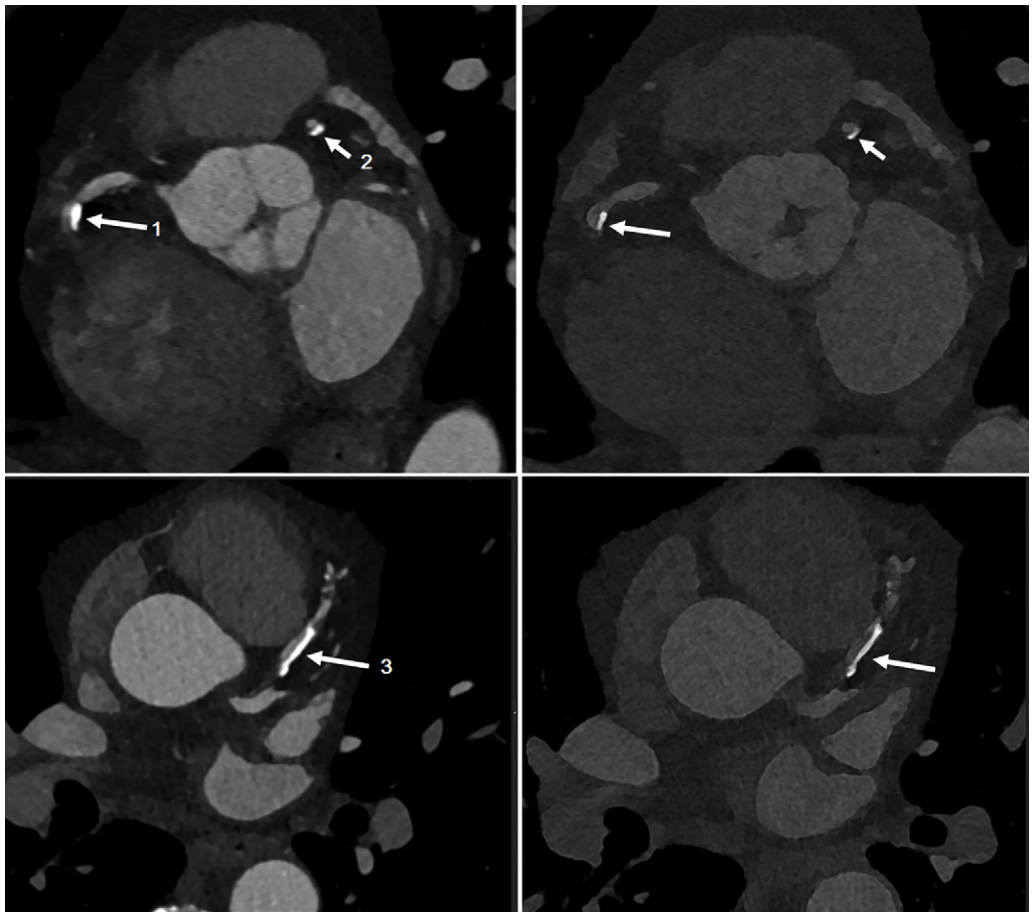


**Figure 3:** Double-oblique short-axis images (top row) and axial images (bottom row) from an energy-integrating detector (EID) CT system (left column) and a photon-counting detector (PCD) CT system at 100 keV (right column) in a 61-year-old male participant referred for clinical coronary CT angiography. Relative to the EID CT images, calcium blooming in the PCD CT images is consistently lower for plaques of different sizes (arrows). The visual percent diameter luminal stenosis estimates for calcifications 1, 2, and 3 were 50%, 20%, and 60%, respectively, based on the EID CT images and 40%, 10%, and 40% based on the PCD CT images. Calcification 1 was in the right coronary artery, calcification 2 was in the proximal left anterior descending coronary artery, and calcification 3 was in the left anterior descending coronary artery. Window width was 500 HU and window level was 1500 HU for EID CT, and window width was 545 HU and window level was 1800 HU for PCD CT.

**Table 2: Descriptive Statistics Related to Visual Estimates of Percent Stenosis by Two Readers**

| Reader | Lesions with ≥30% Stenosis at EID CT* | Percent Diameter Luminal Stenosis | | Mean Difference | $P$ Value† |
|---|---|---|---|---|---|
| | | EID CT | PCD CT | | |
| 1 | 20/39 (51) | Mean ± SD: 37.7 ± 28.5<br>Median: 31.8 (IQR, 12.9–69.7)<br>Range: 0.6–85.3 | Mean ± SD: 32.6 ± 28.0<br>Median: 20.6 (IQR, 8.8–61.2)<br>Range: 0.0–80.0 | −5.1 ± 7.5 | <.001 |
| 2 | 14/32 (44) | Mean ± SD: 37.5 ± 36.3<br>Median: 22.9 (IQR, 1.8–67.4)<br>Range: 0.6–100.0 | Mean ± SD: 30.0 ± 34.9<br>Median: 6.5 (IQR, 0.4–54.1)<br>Range: 0.0–98.2 | −7.4 ± 12.3 | .002 |

Note.—This analysis included lesions with greater than 0% stenosis at EID CT, with a maximum of one lesion per artery. EID = energy-integrating detector, PCD = photon-counting detector.
* Data are numbers of lesions with at least 30% stenosis as a proportion of the numbers of lesions with greater than 0% stenosis, with percentages in parentheses.
† Percent stenosis values at EID CT and PCD CT were compared within readers using the Wilcoxon signed-rank test.

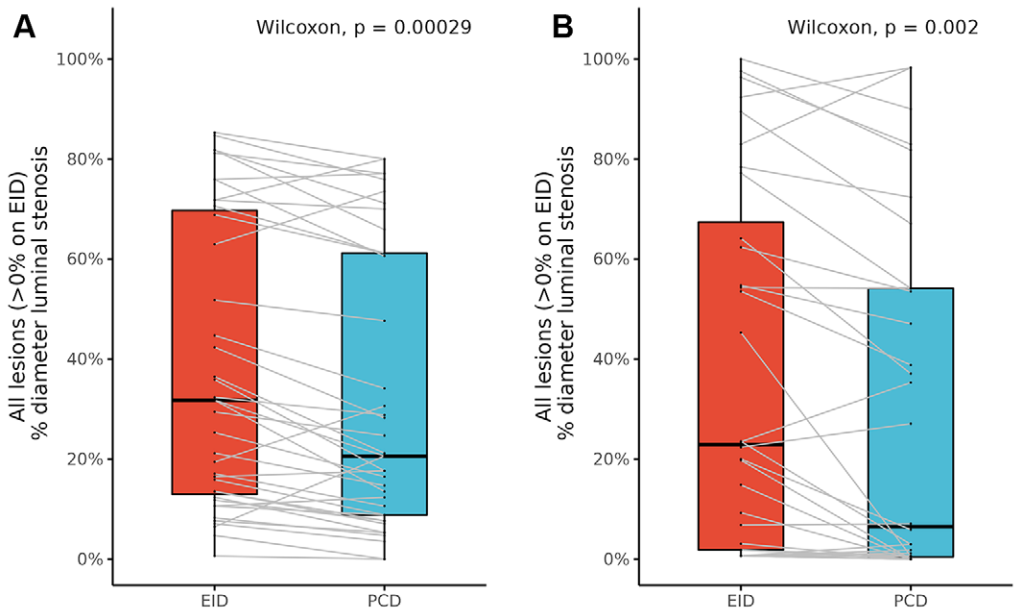


**Figure 4:** Box and whisker plots show paired visual estimates of percent diameter luminal stenosis for a dual-source energy-integrating detector (EID) CT system and a dual-source photon-counting detector (PCD) CT system as assessed by **(A)** reader 1 and **(B)** reader 2. Gray lines represent the paired responses between the two imaging approaches. Horizontal black lines in boxes represent median values, upper and lower bounds of the boxes represent the first and third quartiles, and whiskers represent the range. Visual estimates of percent stenosis at EID CT and PCD CT were compared using the Wilcoxon signed-rank test, which accounted for the pairing in the data.

values and visual ratings based on PCD CT images (mean, 27.9% ± 17.9; median, 22.5% [IQR, 18.1%–35.6%]; $P = .15$).

## Discussion

Compared with energy-integrating detector (EID) CT, the improved resolution of photon-counting detector (PCD) CT coupled with high-energy virtual monoenergetic images (VMIs) has been shown to decrease calcium blooming artifacts on images in phantoms and cadaveric specimens (6,15–19). This study aimed to determine the impact of dual-source PCD CT on the visual and quantitative estimation of percent diameter luminal stenosis compared with dual-source EID CT in participants clinically indicated for cardiac CT. For two readers, median visual estimates of percent stenosis were lower at PCD CT than EID CT (reader 1: 20.6% [IQR, 8.8%–61.2%] vs 31.8% [IQR, 12.9%–69.7%], $P < .001$; reader 2: 6.5% [IQR, 0.4%–54.1%] vs 22.9% [IQR, 1.8%–67.4%], $P = .002$). No difference was observed for quantitative measures of percent stenosis at PCD CT versus EID CT (median difference, −1.5% [95% CI: −3.0%, 2.5%]; $P = .51$). The results reported are consistent with those seen in cadaveric specimens, phantoms, and human subjects (16–22,25). Specifically, calcifications appear smaller on PCD CT images than on EID CT images due to decreased calcium blooming. The decreased blooming on PCD CT images is due to the use of smaller detector pixels, sharper reconstruction kernels, and 100-keV VMIs. Sandstedt et al (17) demonstrated more accurate assessment of ex vivo coronary calcification with PCD CT relative to EID CT when micro-CT was used as ground truth. In a phantom study, Koons et al (16) demonstrated that PCD CT provided a more accurate assessment of coronary luminal stenosis than EID CT due to its high spatial resolution. In the context of coronary CT angiography, Si-Mohamed et al (22) also found that calcified stenotic lesions appeared less severe at PCD CT.

While CAD-RADS scores evaluated at EID CT and PCD CT did not differ for reader 1, reader 2 assigned different scores to examinations in seven of 25 (28%) participants. This change in CAD-RADS scores is similar to findings reported by Rajiah et al (25), who reported that, compared with EID CT, PCD coronary CT angiograms increased reader confidence in the assessment of luminal stenosis in the presence of calcific plaques and resulted in a change of CAD-RADS score in nine of 53 patients. Based on the study by Rajiah et al (25), phantom findings (16), ex vivo studies (17), and the results presented here, a downgrading of CAD-RADS scores due to decreased calcium blooming on images is likely to occur in some patients with the use of PCD CT.

PCD CT images were reconstructed with a sharper reconstruction kernel to take advantage of the inherently better resolution of the PCD system relative to the EID system. Had we reconstructed the PCD CT images at the same sharpness as that of the EID clinical protocol (Bv40), the result would have been lower-noise images, but the cutoff frequency of the Bv40 kernel would have limited the ability to see the "extra" resolution of PCD CT. We could have used a sharper kernel with the EID CT system, but the Bv48 and Bv56 kernels were considered to be too noisy at the current CT dose level for use in our clinical practice. Sharper kernels were used for PCD CT (Bv48 for participants weighing >90 kg and Bv56 for participants weighing ≤90 kg) to improve the point spread function and thereby reduce calcium blooming on images. The noise at these kernels was considered comparable to that of EID CT at Bv40 and acceptable for clinical use.

Quantitative analysis of 18 stenoses that could be clearly matched between EID CT and PCD CT images demonstrated no difference in percent stenosis (mean, 23.8% ± 10.1 vs 23.4% ± 11.9, respectively; $P = .51$). When the same 18 stenoses were graded by the readers, the readings based on EID CT images overestimated percent stenosis compared with the quantitative results, while the readings based on PCD CT images did not. These results suggest that readers tend to overestimate stenosis severity in the presence of blooming artifacts, as with EID CT,

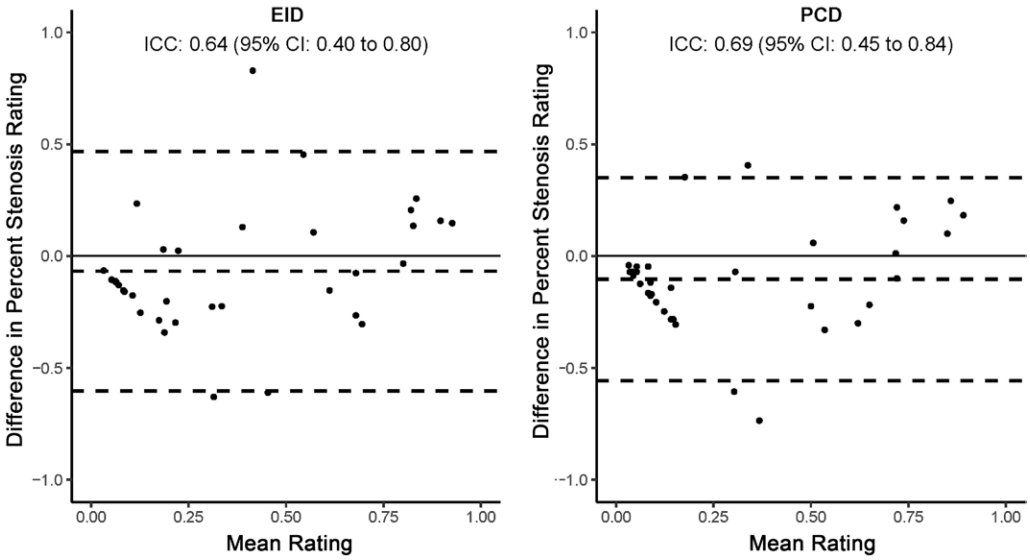


**Figure 5:** Bland-Altman plots show the agreement between readers on visual estimates of percent diameter luminal stenosis on images from a dual-source energy-integrating detector (EID) CT system (left) and dual-source photon-counting detector (PCD) CT system (right) for the 36 lesions where at least one of the two readers graded the percent stenosis as 10% or higher at either EID CT or PCD CT. The intraclass correlation coefficient (ICC) for a two-way random effects model is given at the top of each graph. The mean difference in ratings between the readers (middle dashed line) and the ±1.96-SD limits of agreement (upper and lower dashed lines) are also shown. These values were a mean of −6.8% with limits of −60.3% and 46.7% for EID CT and a mean of −10.3% with limits of −55.6% and 35.0% for PCD CT.

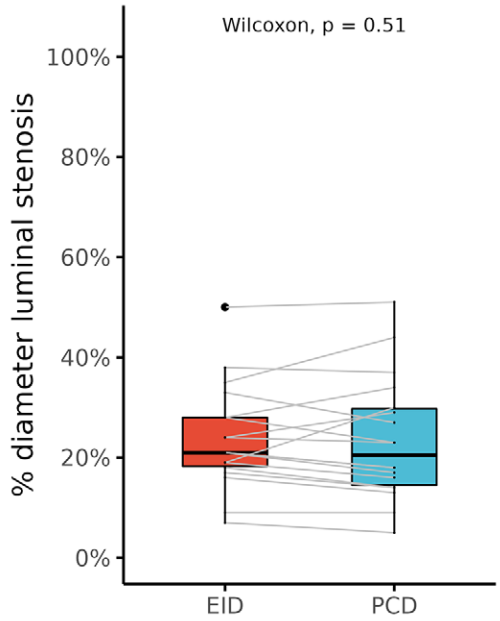


**Figure 6:** Box and whisker plot shows paired quantitative estimates of percent diameter luminal stenosis based on images from a dual-source energy-integrating detector (EID) CT system and a dual-source photon-counting detector (PCD) CT system. Gray lines represent the paired responses between the two imaging approaches. Horizontal black lines in boxes represent median values, upper and lower bounds of the boxes represent the first and third quartiles, and whiskers represent the range. Quantitative estimates of percent stenosis at EID CT and PCD CT were compared using the Wilcoxon signed-rank test, which accounted for the pairing in the data. ● = outlier.

yet provide accurate stenosis severity estimates when the blooming artifacts are substantially reduced, as with PCD CT.

Our study has limitations. First, only 25 participants and two readers were included. A study involving more readers who marked and matched the rated stenoses and including repeat reads to assess intrareader variation would provide important insights into reader variability. Second, the relative impact of the 50-keV versus the 100-keV images was not determined, as the readers were allowed to view both images at the same time. Third, the order of reading was not blinded or randomized. Finally, the clinical impact of these preliminary findings needs to be determined in larger numbers of patients, as a consistent downgrading of CAD-RADS scores at PCD CT versus EID CT could inaccurately imply a change in patient condition between the two examinations.

In conclusion, we showed that photon-counting detector (PCD) CT images at 100 keV demonstrated decreased calcium blooming compared with energy-integrating detector (EID) CT images, resulting in a decrease in the visual estimates of percent diameter luminal stenosis by two readers. That a decrease in visual estimates of percent stenosis, and potential downgrading of Coronary Artery Disease Reporting and Data System score, can occur needs to be taken into account for patients receiving serial coronary CT angiography when the imaging approach used changes from EID CT to PCD CT.

**Acknowledgments:** The authors thank Kevin Kimlinger, BFA, for his assistance with manuscript preparation. The CT system used in this work was provided by Siemens Healthineers.

**Author contributions:** Guarantors of integrity of entire study, **C.H.M., J.P.B.**; study concepts/study design or data acquisition or data analysis/interpretation, all authors; manuscript drafting or manuscript revision for important intellectual content, all authors; approval of final version of submitted manuscript, all authors; agree to ensure any questions related to the work are appropriately resolved, all authors; literature research, **C.H.M., P.R., J.E.T., S.L.**; clinical studies, **C.H.M., P.R., J.P.B., K.R., E.E.W., S.L.**; experimental studies, **E.E.W., J.E.T., S.L.**; statistical analysis, **T.N.W., R.E.C.**; and manuscript editing, **C.H.M., P.R., J.P.B., R.E.C., K.R., J.E.T., S.L.**

**Disclosures of conflicts of interest: C.H.M.** Research grant and in-kind equipment support to institution from Siemens Healthineers; owns intellectual property broadly related to the topic of this article with Mayo Clinic; travel support to attend required collaboration meeting from Siemens Healthineers; served on photon counting CT advisory board for Siemens Healthineers; and board member for the International Society for Computed Tomography. **P.R.** Author and editor services for Elsevier. **J.P.B.**

No relevant relationships. **T.N.W.** No relevant relationships. **R.E.C.** No relevant relationships. **K.R.** No relevant relationships. **E.E.W.** No relevant relationships. **J.E.T.** No relevant relationships. **S.L.** No relevant relationships.

## References


1. Leng S, Bruesewitz M, Tao S, et al. Photon-counting detector CT: system design and clinical applications of an emerging technology. RadioGraphics 2019;39(3):729–743.
2. Rajendran K, Petersilka M, Henning A, et al. First clinical photon-counting detector CT system: technical evaluation. Radiology 2022;303(1):130–138.
3. Willemink MJ, Persson M, Pourmorteza A, Pelc NJ, Fleischmann D. Photon-counting CT: technical principles and clinical prospects. Radiology 2018;289(2):293–312.
4. Flohr T, Petersilka M, Henning A, Ulzheimer S, Ferda J, Schmidt B. Photon-counting CT review. Phys Med 2020;79:126–136.
5. Taguchi K, Iwanczyk JS. Vision 20/20: single photon counting x-ray detectors in medical imaging. Med Phys 2013;40(10):100901.
6. Sandfort V, Persson M, Pourmorteza A, Noël PB, Fleischmann D, Willemink MJ. Spectral photon-counting CT in cardiovascular imaging. J Cardiovasc Comput Tomogr 2021;15(3):218–225.
7. Rajendran K, Petersilka M, Henning A, et al. Full field-of-view, high-resolution, photon-counting detector CT: technical assessment and initial patient experience. Phys Med Biol 2021;66(20):205019.
8. Gutjahr R, Halaweish AF, Yu Z, et al. Human imaging with photon counting-based computed tomography at clinical dose levels: contrast-to-noise ratio and cadaver studies. Invest Radiol 2016;51(7):421–429.
9. Leng S, Rajendran K, Gong H, et al. 150-μm spatial resolution using photon-counting detector computed tomography technology: technical performance and first patient images. Invest Radiol 2018;53(11):655–662.
10. Leng S, Yu Z, Halaweish A, et al. Dose-efficient ultrahigh-resolution scan mode using a photon counting detector computed tomography system. J Med Imaging (Bellingham) 2016;3(4):043504.
11. Abbara S, Blanke P, Maroules CD, et al. SCCT guidelines for the performance and acquisition of coronary computed tomographic angiography: a report of the society of Cardiovascular Computed Tomography Guidelines Committee: endorsed by the North American Society for Cardiovascular Imaging (NASCI). J Cardiovasc Comput Tomogr 2016;10(6):435–449.
12. Writing Committee Members; Gulati M, Levy PD, et al. 2021 AHA/ACC/ASE/CHEST/SAEM/SCCT/SCMR guideline for the evaluation and diagnosis of chest pain: a report of the American College of Cardiology/American Heart Association Joint Committee on Clinical Practice Guidelines. J Am Coll Cardiol 2021;78(22):e187–e285.
13. Dweck MR, Williams MC, Moss AJ, Newby DE, Fayad ZA. Computed tomography and cardiac magnetic resonance in ischemic heart disease. J Am Coll Cardiol 2016;68(20):2201–2216.
14. Sandstedt M, De Geer J, Henriksson L, et al. Long-term prognostic value of coronary computed tomography angiography in chest pain patients. Acta Radiol 2019;60(1):45–53.
15. Marsh JF Jr, VanMeter PD, Rajendran K, Leng S, McCollough CH. *Ex vivo* coronary calcium volume quantification using a high-spatial-resolution clinical photon-counting-detector computed tomography. J Med Imaging (Bellingham) 2023;10(4):043501.
16. Koons E, VanMeter P, Rajendran K, Yu L, McCollough C, Leng S. Improved quantification of coronary artery luminal stenosis in the presence of heavy calcifications using photon-counting detector CT. Proc SPIE Int Soc Opt Eng 2022;12031:120311A.
17. Sandstedt M, Marsh J Jr, Rajendran K, et al. Improved coronary calcification quantification using photon-counting-detector CT: an ex vivo study in cadaveric specimens. Eur Radiol 2021;31(9):6621–6630.
18. VanMeter P, Marsh J Jr, Rajendran K, Leng S, McCollough C. Quantification of coronary calcification using high-resolution photon-counting-detector CT and an image domain denoising algorithm. Proc SPIE Int Soc Opt Eng 2022;12031:120311R.
19. van der Werf NR, Rodesch PA, Si-Mohamed S, et al. Improved coronary calcium detection and quantification with low-dose full field-of-view photon-counting CT: a phantom study. Eur Radiol 2022;32(5):3447–3457.
20. Mergen V, Sartoretti T, Baer-Beck M, et al. Ultra-high-resolution coronary CT angiography with photon-counting detector CT: feasibility and image characterization. Invest Radiol 2022;57(12):780–788.
21. Boccalini S, Si-Mohamed SA, Lacombe H, et al. First in-human results of computed tomography angiography for coronary stent assessment with a spectral photon counting computed tomography. Invest Radiol 2022;57(4):212–221.
22. Si-Mohamed SA, Boccalini S, Lacombe H, et al. Coronary CT angiography with photon-counting CT: first-in-human results. Radiology 2022;303(2):303–313.
23. Albrecht MH, Vogl TJ, Martin SS, et al. Review of clinical applications for virtual monoenergetic dual-energy CT. Radiology 2019;293(2):260–271.
24. Mannelli L, MacDonald L, Mancini M, et al. Dual energy computed tomography quantification of carotid plaques calcification: comparison between monochromatic and polychromatic energies with pathology correlation. Eur Radiol 2015;25(5):1238–1246.
25. Rajiah PS, Dunning CAS, Rajendran K, et al. High-pitch multienergy coronary CT angiography in dual-source photon-counting detector CT scanner at low iodinated contrast dose. Invest Radiol 2023;58(9):681–690.
26. Cury RC, Abbara S, Achenbach S, et al. Coronary Artery Disease - Reporting and Data System (CAD-RADS): an expert consensus document of SCCT, ACR and NASCI: endorsed by the ACC. JACC Cardiovasc Imaging 2016;9(9):1099–1113.
27. Koo TK, Li MY. A guideline of selecting and reporting intraclass correlation coefficients for reliability research. J Chiropr Med 2016;15(2):155–163. [Published correction appears in J Chiropr Med 2017;16(4):346.]